International Journal of Advances in Engineering and Management (IJAEM)
Volume 4, Issue 3 Mar 2022, pp: 1274-1281 www.ijaem.net ISSN: 2395-5252

Flutter simulations on blunt bodies with different turbulence modelling

Yuguang Bai*, Sheng Zhang, Xiaole Xu
School of Aeronautics and Astronautics, Dalian University of Technology, Dalian 116023, China

Submitted: 20-03-2022 Revised: 27-03-2022 Accepted: 30-03-2022

ABSTRACT: Fluid-structure interaction effects have influenced long-span structures significantly. Turbulence effects are also needed to be included. This paper presented series of numerical simulations of the flow around moving blunt bodies with different three dimensional (3D) turbulence models. A classical section of a long-span bridge and an inversed-U shaped beam section are presented with three dimensional CFD modelling and simulations. The fluid-structure interaction effect was solved based on Gauss-Seidel block-iterative coupling algorithm. Flutter derivatives of the two structures are computed and the turbulence flows around them wereanalyzed. Wind tunnel experiments were taken to valid numerical simulation results. It was seen from the computed results that 3D CFD simulations could identify flutter derivatives of long-span structures effectively. The hybrid RANS/LES modelis a good choice versus flutter simulations of blunt body structures with sharp edges. Also, turbulence modelling is necessary for wind effects.

KEYWORDS:long span structures, blunt body, flutter, turbulence modelling.

I. INTRODUCTION

Wind-induced vibration including fluid-structure interaction (FSI) is one of the challenging problems related to long-span structures [1]. Tacoma bridge in USA was damaged due to such phenomena in 1940 when the wind velocity is only 19m/s [2]. It has been seen thatflutter simulations are challenging engineering problems for these kind of structures.

It was recognized that wind tunnel experiments have been the most popular way to test the wind-induced vibration problem, but the cost cannot be taken by most engineers. For the past decades, the power of computers has been increasing continuously and CFD has been recognized as an effective analysis tool for interdisciplinary numerical investigations [3-5].

Transient or steady wind loadings are usually necessary factors for long-span structure designs. An efficient FSI coupling algorithm is necessary and mesh or meshless methods also attract much attention. Tamura and Ono [6] reviewed the state-of-the-art of computational FSI research in the field of wind engineering. The results compared well with experimental measurements, but the computational effort was high due to the usage of Smagorinsky's large eddy simulation (LES) turbulence model. Nomura and Frandsen [7] approached the FSI problem by modelling a two dimensional (2D) laminar flow with the finite element method (FEM). Fairuz et al. [8] presented an investigation into FSI of unsteady aerodynamics of flapping wing at Low Reynolds Number through the multi-physics code coupling interface, using the commercial software FLUENT and ABAQUS solvers. Progress has thus been made for the predictions of the flow aroundblunt bodies. Spalart [2] proposed the advantages of RANS modelling for the computational complexity of 3D CFD studies. Considering the computer power and to decrease the LES resolution requirements, a hybrid RANS/LES model named detached-eddy simulation (DES) was proposed by Spalart et al. [9]. The topic of this model is to solve near-wall flow with RANS modelling and far-wall flow with LES. It can achieve an effective balance between computational complexity and accuracy.

This paper wants to find appropriate 3D turbulence modelling based on CFD method to simulated the flow around blunt body structures related to flutter. RANS, LES and hybrid RANS/LES models are employed based on Gauss-Seidel FSI coupling algorithm and an efficient mesh control method to analyze aerodynamics of two different blunt body structures. Numerical results will be compared to wind tunnel experimental results and the computed values via commercial software. So the usage characteristic of turbulence modelling of streamlined blunt body

International Journal of Advances in Engineering and Management (IJAEM)
Volume 4, Issue 3 Mar 2022, pp: 1274-1281 www.ijaem.net ISSN: 2395-5252

structures and the ones with sharp edges can be concluded.Also the efficiency of the three models will be presented.

II. NUMERICAL ALGORITHM

Coupling Algorithm

This algorithm was developed from one dimensional block-iterative coupling method. For FSI problem, governing equations come from both flow and structural analyses. The discretized incremental Navier–Stokes and structural equations are summarized as [10]:

$\boldsymbol{\vartheta}(a, b) = 0$, $\boldsymbol{\Gamma}(b) = F(a)$ (1)

here a and b are the field vectors that contains the unknowns at the time step n+1 currently being solved for; the discretized velocity vector in the fluid is u; the corresponding pressures is p;and the discretized displacement vector in the structure isη and the corresponding velocityis $\dot{\eta}$; $a = \langle \mathbf{u}^{n+1}, \mathbf{p}^{n+1} \rangle$ contains the variables from the fluid aspect; $b = (\eta^{n+1}, \dot{\eta}^{n+1})$ contains the structural aspect variables. The field variables at the previous time step nare assumed to be known. By this it can fully couple the two equation sets.

Equation (1) can be solved by the block-iterative method [10]. Then the Navier-Stokes equations are solved first for a and then for b. The iteration scheme can be written as

$\boldsymbol{\vartheta}(\mathbf{a}^{(i+1)}, \mathbf{b}^{(i)}) = 0$ (2)

$\boldsymbol{\Gamma}(\mathbf{a}^{(i+1)}) = F(\mathbf{a}^{(i+1)})$ (3)

wherei is the iteration counter and the convergence is linear.

Equations (2) and (3) are both treated as nonlinear. The Newton–Raphson linearization method can be used. Then linearization iteration is

$\mathbf{a}_{(j+1)}^{(i+1)} = M(\mathbf{a}_{(j)}^{(i+1)}, \mathbf{b}^{(i)})$ (4)

$\mathbf{b}_{(j+1)}^{(i+1)} = N(\mathbf{a}^{(i+1)}, \mathbf{b}_{(j)}^{(i+1)})$ (5)

where j is the linearization iteration counter. The two layers of iteration i and j in Equations (4)and (5) include both the non-linearity and the field coupling. With global convergence checked at every time step, the solution obtained should be identical to that given by the direct coupled solution to Equations (2) and (3). After being merged the equivalent iteration can be written as

$\mathbf{a}^{(k+1)} = M(\mathbf{a}^{(k)}, \mathbf{b}^{(k)})$ (6)

$\mathbf{b}^{(k+1)} = N(\mathbf{a}^{(k+1)}, \mathbf{b}^{(k)})$ (7)

where k is the merged iteration counter. Solvers in the form of Equations (6) and (7) can be applied with existing CFD and structural analysis codes.

Turbulence model used

There are some popular turbulence models for CFD computations. Many works have discussed advantages and disadvantages of them [3-8].

Unsteady RANS models are still the most popular in industrial application, especially for aeronautical engineering related to initial evaluations of aircraft aerodynamics.

There are two main models for RANS:$k-\varepsilon$ and $k-\omega$. Fork $-\varepsilon$ model, the transport equations for turbulent kinetic energy k and its dissipation rate ε are given by the following equations in which the five constants needed are given the values of $\sigma_k = 1.0$, $\sigma_\varepsilon = 1.3$, $C_\nu = 0.09$, $C_{1\varepsilon} = 1.44$, and $C_{2\varepsilon} = 1.92$[9].

$$\frac{\partial}{\partial t}(\rho k) + \frac{\partial}{\partial x_i}(\rho k u_i) = \frac{\partial}{\partial x_i}\left[\left(\nu + \frac{\nu_t}{\sigma_k}\right)\frac{\partial k}{\partial x_i}\right] + G_k - Y_k \quad (8)$$

$$\frac{\partial}{\partial t}(\rho \varepsilon) + \frac{\partial}{\partial x_i}(\rho \varepsilon u_i) = \frac{\partial}{\partial x_i}\left[\left(\nu + \frac{\nu_t}{\sigma_\varepsilon}\right)\frac{\partial \varepsilon}{\partial x_i}\right] + G_\varepsilon - Y_\varepsilon \quad (9)$$

LES was proposed for eddy simulations. The filtered Navier–Stokes equations for a constant density fluid can be obtained from the Equation (10):

$$\frac{\partial \rho \bar{u}_i}{\partial t} + \frac{\partial \rho \bar{u}_i \bar{u}_j}{\partial x_j} = -\frac{\partial \bar{p}}{\partial x_i} + 2\frac{\partial (\eta_t \bar{S}_{ij})}{\partial x_j} - \frac{\partial \tau_{ij}}{\partial x_j} \quad (10)$$

where ν_t is the sub-grid eddy viscosity and $\overline{S_{ij}}$ is the rate-of-strain tensor calculated with the filtered velocity components. The sub-grid eddy viscosity has to be further modeled. The isotropic part of the stresses is not modeled but added to the pressure term.

With different kinds of RANS models, DES models have two kinds. The first is the DES k-ε model. The transport equations for k and ε of the realizable k-ε model are used to model the eddy viscosity in the RANS zones and to model the sub-grid viscosity in the LES zones. In the hybrid formulation, the dissipation term in Equation (8) is computed from

$$Y_k = \rho k^{3/2}/\ell_{des} \quad (11)$$

where $\ell_{des} = \min(\ell_{rke}, \ell_{les})$, $\ell_{rke} = k^{3/2}/\varepsilon$, $\ell_{les} = C_{des}\Delta$ and $\Delta = \max(\Delta x, \Delta y, \Delta z)$, the maximum grid spacing. The standard value of C_{des} is 0.65 [9].

The second isthe DES k-ω model. The dissipation term of the turbulent kinetic energy is modified into Equation (11), where $\ell_{des} = \min(\ell_{k\omega}, \ell_{les})$, $\ell_{k\omega} = k^{1/2}/\beta^*\omega$ and $\ell_{les} = C_{des}\Delta$, as in the previous model.

For blunt body like structures with sharp edges, eddy simulations are recognized to be necessary. It is seen that if unnecessary use for flows that RANS or LES can handle, also it is in terms of computational accuracy and efficiency, DES is a very good choice.For the detail situation of each kind of turbulence models, the k-ω SST RANS model has some advantages than the k-ε RANS model: the k-ε model does not allow direct

International Journal of Advances in Engineering and Management (IJAEM)
Volume 4, Issue 3 Mar 2022, pp: 1274-1281 www.ijaem.net ISSN: 2395-5252

integration through the boundary layer and also produces excessive turbulence kinetic energy at impingement on the wall, which may significantly affect the flow patterns; and in contrast, the k-ω model allows direct integration through the boundary layer. The DES k-ω SST model is thus used in this paper to keep relevance.

III. STRUCTURES AND MESH GENERATION

This Paper used two structures, as shown in Figure 1. The first one is a classical cross section of long-span Bridge, see Figure 1(a). This structure has been used in the designs of many long-span bridge over the world. It was considered as a streamlined blunt body. The second one is an inverse-U shaped beam, see Figure 1(b). A wind tunnel experiment was accomplished with it,see Figure 1(c). It is a blunt body with sharp edges, For the cross section of Tsing Ma bridge, this paper used a reduced scale of the real structure. The chord length B is given a value of 1m, see Figure 1(a). The length (i.e. perpendicular to the section shown on Figure 2) L is also equal to 1m. For the inverse-U shaped beam, B=0.7m and L= 0.7m according to the experiment, as shown in Figure 1(b) (i.e. the unit in Figure 1(b) is cm).

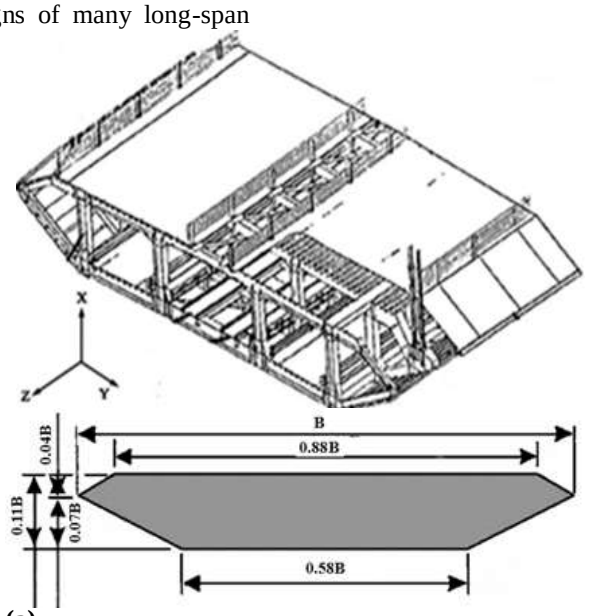

(a)

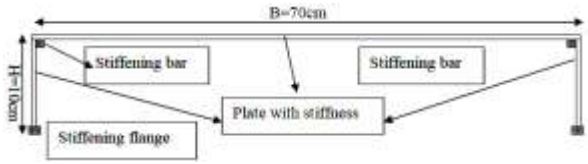

(b)

(c)

Figure1. Structure basements [11]

International Journal of Advances in Engineering and Management (IJAEM)
Volume 4, Issue 3 Mar 2022, pp: 1274-1281 www.ijaem.net ISSN: 2395-5252

Mesh generation in this paper makes use of the rigid plane assumption fundamental in classical beam theories [10]. The cylinder region under consideration is divided into a rigid region with R≤R1and a buffer region with R1<R≤R2, see Figure 2(a). Fluid grids in the rigid region are assumed to translate and rotate in the rigid plane. Grids falling in the buffer region are updated with mesh movements that are interpolated from those at R=R1 and R=R2.

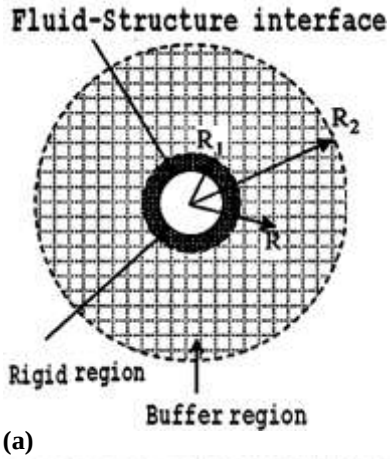

(a)

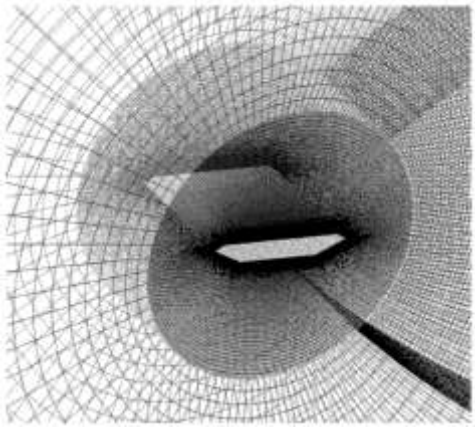

(b)

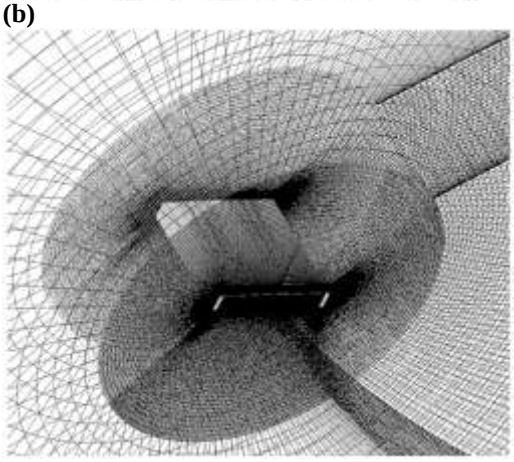

(c)

Figure 2. Mesh generation

Total meshes of the classical bridge section and the U beam are 3,400 thousand and 2,433 thousand, respectively. Mesh independence tests were taken through different meshes of RANS and DES to valid that workable meshes could be found.

International Journal of Advances in Engineering and Management (IJAEM)
Volume 4, Issue 3 Mar 2022, pp: 1274-1281 www.ijaem.net ISSN: 2395-5252

IV. FLUTTER COMPUTATION

Flutter derivatives computational method

Flutter is one of the most important aeroelastic phenomena for long-span structures. Flutter derivative evaluate approach is widely used to estimate flutter critical velocity of long-span bridges. The formula using flutter derivative for bridge decks has its root from Theodorsen theory. Unsteady aeroelastic force can be expressed as a linear combination of deck motions using 8 flutter derivatives [12]. Each of them is a function of the reduced flow frequency K=ωB⁄U. So the reduced velocity of flow is changed by changing the frequency of forced vibration, rather than changing the velocity of wind flow.

$$L_{ae} = \frac{1}{2}\rho U^2 B[KH_1^*\frac{\dot{h}}{U} + KH_2^*\frac{B\dot{\alpha}}{U} + K^2H_3^*\alpha + K^2H_4^*]$$

$$A_1^* = -\frac{\overline{M_h(t)}\sin\phi}{h_0K^2\rho U^2B}, A_2^* = \frac{\overline{M_\alpha(t)}\sin\phi}{\alpha_0K^2\rho U^2B^2}$$
$$A_3^* = \frac{\overline{M_\alpha(t)}\cos\phi}{\alpha_0K^2\rho U^2B^2}, A_4^* = \frac{\overline{M_h(t)}\cos\phi}{h_0K^2\rho U^2B} \quad (14)$$
$$H_1^* = -\frac{\overline{L_h(t)}\sin\phi}{h_0K^2\rho U^2}, H_2^* = -\frac{\overline{L_\alpha(t)}\sin\phi}{\alpha_0K^2\rho U^2B}$$
$$H_3^* = \frac{\overline{L_\alpha(t)}\cos\phi}{\alpha_0K^2\rho U^2B}, H_4^* = \frac{\overline{L_h(t)}\cos\phi}{h_0K^2\rho U^2}$$

where $\overline{L_i}$ and $\overline{M_i}$ are, respectively, mean values of the section lift and section moment caused by the forced vertical (i = h) and twisting (i = α) vibration. Thus, A_1^*, A_4^*, H_1^* and H_4^* can be computed from the forced vertical motion, and A_2^*, A_3^*, H_2^* and H_3^* can be computed from the forced twisting motion.

Computational results of flutter derivatives

Forced motion simulations are conducted by using the driving signal amplitudes of Equation (14) with $h(t) = 0.05B\sin\omega t$ and $\alpha(t) = 3\sin\omega t$. Each individual simulation should be run for enough time increments for the simulated time traces of $\overline{L_i}$ and $\overline{M_i}$ to be stable. The analysis of the simulations involved the least-squares fitting of a sinusoid to the simulated $\overline{L_i}$ and $\overline{M_i}$ time traces. An example of this procedure is shown in Figure 7, obtained for the U beam with $\alpha_0 = 3°$ and K = 2.592and 5.671. The flow velocity is still 8m/s and the flow density is 1.225kg/m3. Computational results are shown in Tables 1-4. A_2^*, A_3^*, H_2^* and H_3^* can be obtained via $\alpha_0 = 3°$ and K = 2.592 and 5.671. A_1^*, A_4^*, H_1^* and H_4^* can be obtained via $h_0 = 0.05B$and K = 2.25 and 4.482.

(12)

$$M_{ae} = \rho U^2B^2[KA_1^*\frac{\dot{h}}{U} + KA_2^*\frac{B\dot{\alpha}}{U} + K^2A_3^*\alpha + K^2A_4^*\frac{h}{B}] \quad (13)$$

here h, $\dot{h}$, α and $\dot{\alpha}$ are the vertical and torsional displacements and velocities of deck. H_i^* and A_i^* $(i = 1,\ldots,6)$ are the flutter derivatives. $\omega_i = 2\pi f_i$; f_i are the forced vibration frequencies $(i = h, \alpha)$. The forced vibration was assumed to be of the form

$$h(t) = h_0\, exp(i\omega t), \alpha(t) = \alpha_0\, exp(i\omega t) \quad (14)$$

The motion induced forces are also assumed to be harmonic, with identical ω but a phase shift ϕ relative to the motion. Replacing $exp(-i\phi)$ by $(\cos\phi - i\sin\phi)$ to determine the flutter derivatives from Equations (12) and (13) gives:

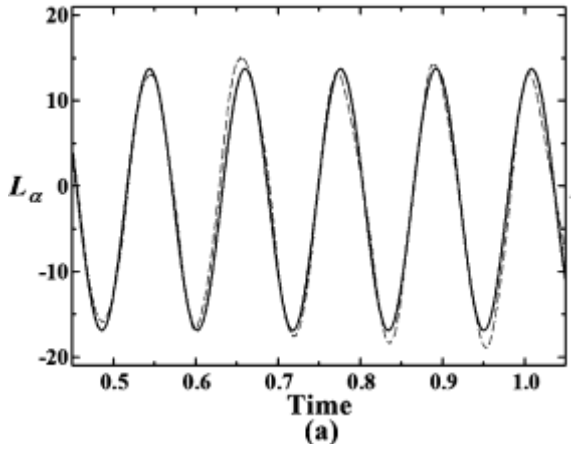

International Journal of Advances in Engineering and Management (IJAEM)
Volume 4, Issue 3 Mar 2022, pp: 1274-1281 www.ijaem.net ISSN: 2395-5252

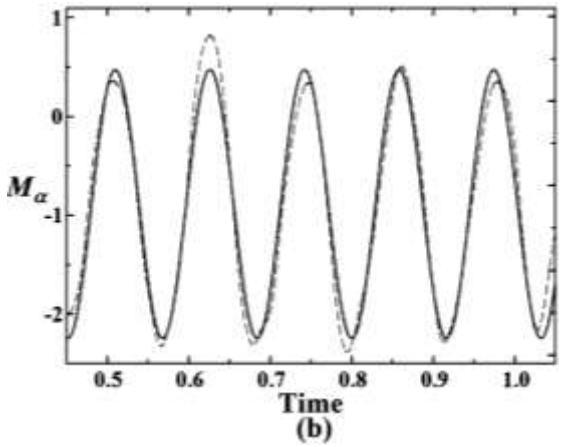

Figure 3. 3D DES simulated motion-induced aerodynamic force time traces (----) and corresponding sinusoidal least-squares fit (solid curve), with $\alpha_0 = 3°$ and K=5.671.

It is seen that for the flutter derivatives, DES simulations with the current numerical method can obtain better results compared to the experimental results than those via 3D RANS simulations. When using (CS = Commercial software), the results are al-so better that 3D RANS simulations. For the U Beam, 3D DES simulations with the current method can obtain good agreements with wind tunnel experiments. The RANS modelling is not successful to be applied when obtaining flutter derivatives.

Flow features

Due to force motion, the transient turbulence structures have much transient variation (i.e. backup result files of four different timesteps for one kind of force motion on the U beam were chosen to view the flow features, as shown in Figure 4). Here mainly present the turbulence structures via DES turbulence modelling.

It is seen that flow structures around the U Beam are very instable. FSI effects are obvious and non-ignorable. The flow structures present massive separation when forced motion are applied on such blunt body. Vortex induced forces on such structures demand effective flow eddy simulation method, So DES modelling is necessary for the flutter prediction of long-span structures. Though 3D simulation is used, RANS cannot be employed for flutter computations for blunt body structures.

Computational efficiency

The comparison of the computational efficiency is shown in Table 5. It is seen that simulations with LES model have the most computational demands. With the proposed coupling algorithm and the mesh control method, the computational cost can be decreased significantly than that of commercial software. Especially for 3D CFD simulations with DES or LES models, the current numerical method can achieve better computed results with less computational times.

Table 1. Computational results of flutter derivatives A_2^* and A_3^*(CS = Commercial software).

Results	A_2^*(K=2.592)	A_2^* (K=5.671)	A_3^* (K=2.592)	A_3^*(K=5.671)
Wind tunnel	-0.068	-0.008	0.051	0.050
RANS	0.013	-0.018	0.012	0.041
DES	-0.075	-0.011	0.048	0.047
CS (DES)	-0.077	-0.013	0.045	0.046

Table 2. Computational results of flutter derivatives H_2^* and H_3^* (CS = Commercial software).

Results	H_2^*(K=2.592)	H_2^* (K=5.671)	H_3^* (K=2.592)	H_3^*(K=5.671)
Wind tunnel	-0.068	-0.008	0.051	0.050
RANS	0.013	-0.018	0.012	0.041
DES	-0.075	-0.011	0.048	0.047
CS (DES)	-0.077	-0.013	0.045	0.046

International Journal of Advances in Engineering and Management (IJAEM)
Volume 4, Issue 3 Mar 2022, pp: 1274-1281 www.ijaem.net ISSN: 2395-5252

Table 3. Computational results of flutter derivatives A_1^* and A_4^* (CS = Commercial software).

Results	A_1^*(K=2.25)	A_1^* (K=4.482)	A_4^* (K=2.25)	A_4^*(K=4.482)
Wind tunnel	0.113	-0.240	-0.409	-0.019
RANS	0.215	0.083	0.113	-0.234
DES	0.111	-0.251	-0.413	-0.235
CS (DES)	0.11	-0.255	-0.415	-0.238

Table 4. Computational results of flutter derivatives H_1^* and H_4^* (CS = Commercial software).

Results	H_1^*(K=2.25)	H_1^* (K=4.482)	H_4^* (K=2.25)	H_4^*(K=4.482)
Wind tunnel	0.059	0.004	0.009	0.034
RANS	-0.043	-0.018	-0.053	0.103
DES	0.085	0.019	0.004	0.007
CS (DES)	0.091	0.017	0.004	0.046

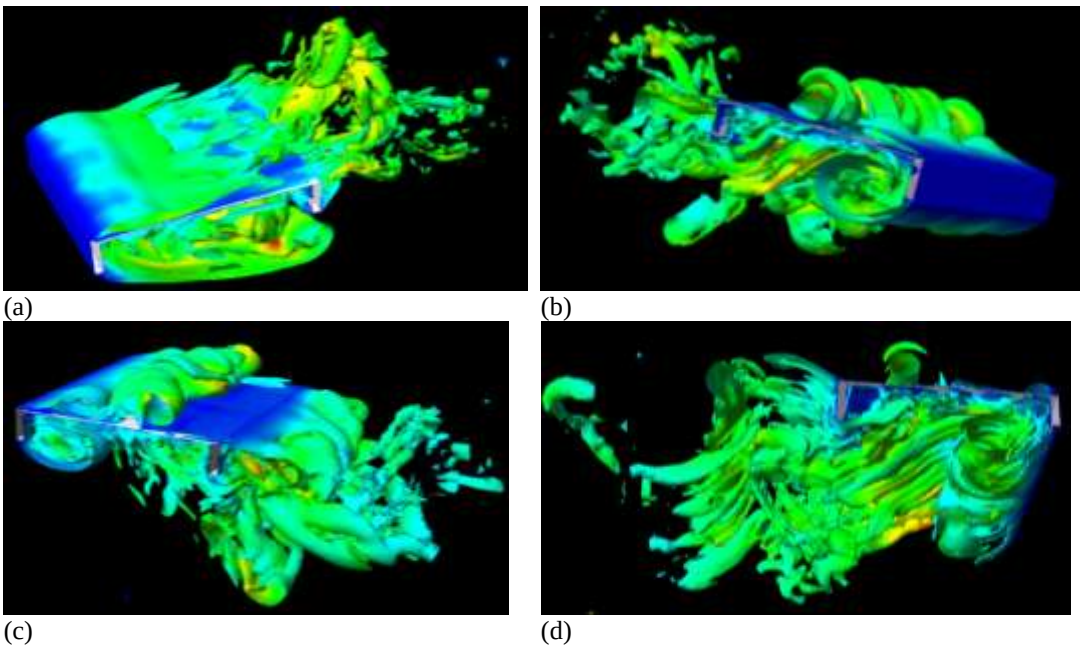

(a) (b) (c) (d)

Figure 4. Four steps of transcient flow structures when force motion is applied on the U beam. (i.e. in these figures, pressure distributions were plotted on an isosurface based on turbulence kinetic energy distributions with a consistent value in the fluid domain.)

Table 5. Comparisons of the computational efficiency with same time steps 50000 (Unit: hours).

	structure	Current numerical method	Commercial software
RANS	Bridge	215	273
	U Beam	193	249
DES	Bridge	399	462
	U Beam	367	431
LES	Bridge	1020	1690
	U Beam	856	1439

V. CONCLUSION

Flutter characteristics of both aclassical blunt body section related to long-span structures and a blunt body structure named inverse-U shaped beam are simulated in this paper. The three main turbulence models are discussed based on CFD method. FSI effect is included with a Gauss-Seidel block-iterative coupling algorithm and an mesh control method. Flutter derivatives are computed from the current numerical method with RANS, LES and DES turbulence models. The computed results are compared with the wind tunnel experimental results and the computed values of the commercial software. Flutter simulations

around the moving structures for different turbulence modelling are analysed. Comparisons of the computational efficiency are also presented.

It can be concluded that:

(1) For the computations of flutter derivatives, no matter the blunt body structure like the cross section of classical long-span bridge or such body with sharp edges, 3D CFD numerical simulations with vortex models are necessary. Though with coupling algorithm and mesh control method, 3D DES simulations are needed at least.

(2) for flutter computations, 3D CFD numerical simulations with hybrid turbulence modelling can obtain satisfactory results with balanced computational demands than those with LES;

(3) Flutter features around the structure with sharp edges are very complex. Many flow separations occur and appropriate 3D turbulence models are necessary to capture such phenomenon.

Flutter computation analysis in this paper can be usedin the applications of long-span structures with different kinds of cross sections, which can provide important basement for the usage of effective turbulence modelling and numerical analysis faced to wind engineering and civil engineering.

REFERENCES

[1]. Nieto, F.; Hargreaves, D.M.; Owen, J.S.; Hernandez, S.,2015,"On the applicability of 2D URANS and SST k-ω turbulence model to the fluid-structure interaction of rectangular cylinders," Engineering Applications of Computational Fluid Mechanics, 9(1): 157-173.

[2]. Sarkar, P. P.; Caracoglia, L.; Haan, F.L.; Satoc, H.; Murakoshi, J., 2009,"Comparative and sensitivity study of flutter derivatives of selected bridge deck sections: Part 1. Analysis of inter-laboratory experimental data," Engineering Structures, 31(1): 158-169.

[3]. Mavriplis, C., 2012,"Interdisciplinary CFD," International Journal of Computational Fluid Dynamics, 26(6-8): 333-335.

[4]. Cid Montoya, M.; Nieto, F.; Álvarez, A.J.; Hernández, S.; Jurado, J.Á.; Sánchez, R., 2018,"Numerical simulations of the aerodynamic response of circular segments with different corner angles by means of 2D URANS. Impact of turbulence modeling approaches," Engineering Applications of Computational Fluid Mechanics, 12(1): 750-779.

[5]. Benarafa, Y.; Cioni, O.; Ducros, F.; Sagaut, P.,2006,"Rans/les coupling for unsteady turbulent flow simulation at high reynolds number on coarse meshes," Computer Methods in Applied Mechanics & Engineering, 195(23/24): 2939-2960.

[6]. Tamura, T.; Itoh, Y., 1999,"Unstable oscillation of rectangular cylinder at various mass ratios," Journal of Aerospace Engineering, 12(4): 136-144.

[7]. Nomura, T., 1993. A numerical study on vortex-excited oscillations of bluff cylinders. Journal of Wind Engineering and Industrial Aerodynamics, 50(1-3):75–84.

[8]. Fairuz, Z. M., Abdullah, M. Z, Yusoff, H, Abdullah, M. K., 2013,"Fluid Structure Interaction of Unsteady Aerodynamics of Flapping Wing at Low Reynolds Number," Engineering Applications of Computational Fluid Mechanics, 7(1):144-158.

[9]. Spalart, P. R.; Jou, W. H.; Strelets, M.; Allmaras, S. R., 1997,"Comments on the feasibility of LES for wings, and on a hybrid RANS/LES approach" In: Advances in DNS/LES, Greyden Press, 1997, pp.137-147.

[10]. Bai, Y. G.; Sun, D. K.; Lin, J. H. Three dimensional numerical simulations of long-span bridge aerodynamics, using block-iterative coupling and DES. Computers & Fluids 2010, 39(9), 1549-1561.

[11]. Bai, Y. G., Zhang, S., Xu, X. L.,2022, "Numerical investigation on the flow around blunt bodies with different turbulence modeling," International Journal of Research in Engineering and Science, 10(3): 51-58.

[12]. Frandsen, J.B.,2004, "Numerical bridge deck studies using finite elements," Journal of Fluids and Structures, 19: 171-191.

[13]. Bai Y. G., Wu G. Q., Zhang Y. G. A novel parallel computing method for computational fluid dynamics. International Journal of Computer Science Issues, 2013, 10(1), 693-698.